



# Scale locality of helicity cascade in physical space

Cite as: Phys. Fluids **32**, 061705 (2020); <https://doi.org/10.1063/5.0013009>

Submitted: 07 May 2020 . Accepted: 03 June 2020 . Published Online: 16 June 2020

Zheng Yan (闫政) , Xinliang Li (李新亮), and Changping Yu (于长平) 



View Online



Export Citation



CrossMark

## ARTICLES YOU MAY BE INTERESTED IN

[Acoustic-wave-induced cooling in onset of hypersonic turbulence](#)

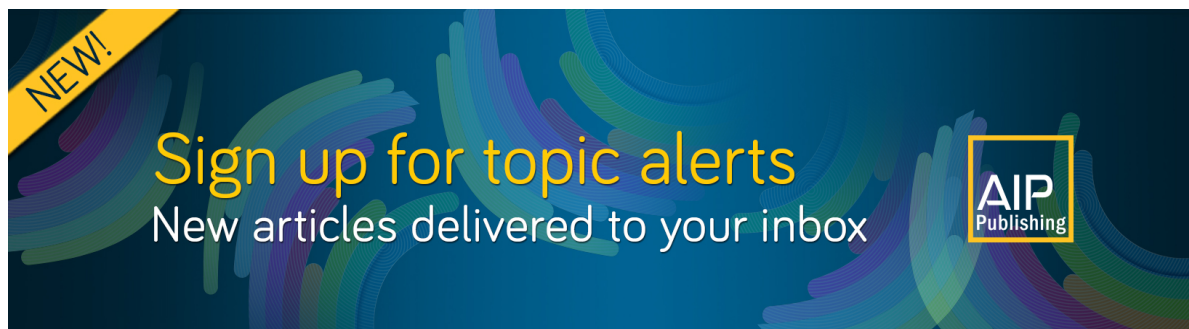
Physics of Fluids **32**, 061702 (2020); <https://doi.org/10.1063/5.0011871>

[Likelihood of survival of coronavirus in a respiratory droplet deposited on a solid surface](#)

Physics of Fluids **32**, 061704 (2020); <https://doi.org/10.1063/5.0012009>

[Dual vortex breakdown in a two-fluid confined flow](#)

Physics of Fluids **32**, 061706 (2020); <https://doi.org/10.1063/5.0012156>





# Scale locality of helicity cascade in physical space

Cite as: Phys. Fluids 32, 061705 (2020); doi: 10.1063/5.0013009

Submitted: 7 May 2020 • Accepted: 3 June 2020 •

Published Online: 16 June 2020



Zheng Yan (闫政),<sup>1,2</sup>  Xinliang Li (李新亮),<sup>1,2</sup> and Changping Yu (于长平)<sup>1,2,a)</sup> 

## AFFILIATIONS

<sup>1</sup>LHD, Institute of Mechanics, Chinese Academy of Sciences, Beijing 100190, China

<sup>2</sup>School of Engineering Science, University of Chinese Academy of Sciences, Beijing 100049, China

<sup>a)</sup> Author to whom correspondence should be addressed: cpyu@imech.ac.cn

## ABSTRACT

Scale locality is a key concept in turbulent cascade theory and is also associated with reflection symmetry. Vortex stretching is proven to participate in the helicity cascade process while destroying the conservative characteristic of enstrophy transfer in three-dimensional flows. Numerical evidence indicates that a turbulent structure with scale  $L$  will also largely transfer its helicity to structures with scales of around  $0.3L$ . However, the scale locality of the helicity cascade is slightly weaker than that of the energy cascade in physical space. The weaker scale locality suggests that more scales should be involved for turbulent modeling of helical turbulence.

Published under license by AIP Publishing. <https://doi.org/10.1063/5.0013009>

The classical turbulent cascade picture describes the successive energy transfer from large scales to small scales, with the energy eventually dissipated by viscosity in the dissipation regions. The key idea involves the scale locality, whereby only neighboring scales make a main contribution to the turbulent cascade.<sup>1</sup> In 1941, Kolmogorov argued that the energy cascade should be local and that the vortex of a specific scale should successively receive energy and transfer it to the next lower order.<sup>2</sup> However, the first quantitative scale-locality results were obtained by Kraichnan in 1959 using the Direct Interaction Approximation (DIA).<sup>3</sup> The locality of the turbulent cascade determines the universal statistics of small scales, which are protected from the influence of larger scales.

Helicity is the integral of the scalar product of velocity  $\mathbf{u}$  and vorticity  $\boldsymbol{\omega}$  and, together with energy, is one of only two inviscid quadratic invariants in three-dimensional turbulent flows. Helicity measures the degree of reflection symmetry and the linkage of vortex lines in the flow field.<sup>4</sup> The successive helicity transfer also requires the scale locality of triadic interactions. This scale locality has been numerically and theoretically verified.<sup>5–16</sup> Yeung and Brasseur<sup>5</sup> provided numerical results at the Taylor microscale Reynolds number of 32 to show that there exist distant triadic interactions coupling energy-containing, which is different from the classical statistical independence between large-scale and small-scale structure. Domaradzki, Liu, and Brachet<sup>6</sup> found that the subgrid-scale transfer

process is dominated in the vicinity of the cutoff wave number and the modes greater than twice the cutoff wave number cannot affect the subgrid-scale process. Local interactions dominate the total energy flux asymptotically, and there exist cancellations among large-amplitude nonlocal interactions.<sup>7</sup> Three specific filters (sharp spectral, Gaussian, and tangent hyperbolic) are used to define the scales of motion, and Domaradzki and Carati<sup>8</sup> found that only a minor dependence on the filter type exists. Onsager's assertion that local triadic interactions dominate the energy cascade in Hölder's solution with the exponent ranged from zero to one has been proven under a stronger Hölder condition.<sup>9</sup> A filtering approach in physical space can also be used to explore the scale locality and energy transfer process in turbulent flows.<sup>10,11,17–19</sup> Through an exact analysis of the governing equations, sufficient conditions established for the locality of turbulent cascades were found to require Hölder continuity but non-differentiability in space.<sup>10</sup> The large-scale velocity and vorticity gradients possess ultraviolet locality, and the small-scale stress possesses infrared locality. In contrast to the energy cascade, the scale locality of the helicity cascade requires more smoothness in the filter function. This method has been applied to a multi-scale gradient expansion of the turbulent stress tensor, which involved the neighboring contributions from different scales of motion and space derivatives of velocity.<sup>11</sup> Verma *et al.*<sup>12</sup> thought that the shell-to-shell energy transfer is local, and the main reason lies in the fact that local

triads occupy much more Fourier space volume. Alexakis, Mininni, and Pouquet<sup>13</sup> studied the scale locality on a grid of  $1024^3$  points and concluded that the nonlinear transfer itself is local, while the interactions with large scales occupy 20% of the total energy flux. Then, Mininni, Alexakis, and Pouquet<sup>14</sup> showed that the nonlocal interactions would weaken with Reynolds number increases through the scaling of the nonlocal energy fluxes. Cardesa *et al.*<sup>15</sup> and Cardesa, Vela-Martín, and Jiménez<sup>16</sup> investigated the time evolution of the energy cascade and tracked the flow regions in different scales to verify the scale locality of the energy cascade. The scale locality was also widely explored in magnetohydrodynamic turbulence<sup>20,21</sup> and compressible turbulence.<sup>22</sup>

The locality of turbulent cascades analyzed in wave number space indicates that the energy transfer is dominated by local triadic interactions, which has been verified by smooth coarse-graining and sharp spectral filters in both space and scale.<sup>23,24</sup> The wave number can be substituted for the physical length scale, and the scale locality corresponds to interactions among neighboring wave numbers. A diagrammatic perturbation approach in quasi-Lagrangian variables was used to study the scale locality in wave number space, and an exact relation was established between the asymptotic behaviors of the triadic interactions for energy flux and the double-correlation function for energy distribution.<sup>25</sup> The scale disparity parameter  $s$  was defined to incorporate scaling  $s^{-4/3}$  using classical theory predictions, and the results of direct numerical simulations (DNSs) support the prediction that the interactions are local in the inertial subrange and nonlocal in the dissipation range.<sup>26–28</sup>

The two-point velocity correlation transport and the Karman–Howarth equation were used to analyze the energy cascade in physical space,<sup>29</sup> and the two-point velocity–vorticity correlations have been applied to the evolution of helicity.<sup>30</sup> The quasi-normal-type notation is needed to close the Karman–Howarth equation, which assumes that the joint probability density function of the two-point velocity is Gaussian for fourth-order velocity correlations.<sup>1</sup> The above approximation assumption is inherently arbitrary. Nevertheless, from the perspective of vortex stretching,<sup>11,31</sup> DNS and experiments have confirmed the preferential alignments of vorticity and the intermediate strain rate, which supports the scale locality of straining associated with the self-induced strain fields.<sup>32–34</sup> There is clear numerical evidence for the energy cascade in incompressible homogeneous and isotropic turbulence (HIT) using physical space quantities.<sup>35</sup> A bandpass filter was used to induce turbulent structures with specific scales, and the fluxes between these scales were determined.

There have also been efforts to study the scale locality and properties of helicity in physical space in three-dimensional turbulent flows.<sup>10,11,30,36</sup> Based on a filtering approach, the helicity cascade is believed to possess both the infrared and the ultraviolet locality.<sup>10,11</sup> The finiteness of helicity dissipation was explored using the lack of reflection symmetry of small scales, which is the consequence of nonlocality and conflicts with Kolmogorov’s hypothesis of reflection symmetry at small scales.<sup>36</sup> Velocity–vorticity correlation functions are not invariant under reflection symmetry in physical space, and the reflection symmetry is gradually recovered at small scales.<sup>30</sup>

Hence, there exists a contradiction between scale locality and reflection symmetry in helical turbulence. We can infer that the energy cascade would be less local under the influence of broken reflection symmetry, and the helicity cascade would also be less

local in scale in contrast to the energy cascade because of the more stringent locality condition of the vorticity gradient.<sup>10</sup> However, the direct numerical evidences for the scale locality of energy and helicity cascades in helical turbulence are vacant, and so we try to analyze these concepts in physical space.

The following incompressible Navier–Stokes equations are numerically solved by the pseudo-spectral solver, with a second-order Adams–Bashforth scheme for time integration:

$$\partial \mathbf{u} / \partial t + (\mathbf{u} \cdot \nabla) \mathbf{u} = -\nabla(p/\rho) + \nu \nabla^2 \mathbf{u} + \mathbf{f}, \quad (1)$$

where  $\mathbf{u}$  is the velocity,  $p$  is the pressure,  $\rho$  is the density that is assumed to be constant, and  $\mathbf{f}$  is the external forcing for inputting energy and helicity. The specific form of external forcing can be constructed as a linear combination of velocity  $\mathbf{u}$  and vorticity  $\boldsymbol{\omega}$  as follows:

$$\mathbf{f} = \alpha \mathbf{u} + \beta \boldsymbol{\omega}, \quad (2)$$

where  $\alpha$  and  $\beta$  are two indeterminate dimensional parameters,<sup>37</sup> and the velocity  $\mathbf{u}$  and vorticity  $\boldsymbol{\omega}$  we adopted in our numerical simulations are limited within the lowest two wave number shells. The domain size is within a cubic box with sides of  $2\pi$ , with periodic boundary conditions of three directions. The inputting rates of energy  $\varepsilon = 0.1$  and helicity  $\delta = 0.3$  are employed within the lowest two wave number shells. Some characteristic parameters are summarized in Table I, and for their definitions, refer to our previous paper.<sup>38</sup> In Fig. 1, we supply the time evolution of the mean energy and the mean helicity, and the time is nondimensionalized by the initial large-eddy turnover time. We can see that the flow field reaches a statistical stationary status when the normalized time  $t/\tau_0$  is larger than 25.0, and then we began our numerical analysis.

The power-law solutions of kinetic energy and helicity, which ignores any intermittency corrections,<sup>39</sup> can be written as

$$E(k) \sim C_E \varepsilon^{2/3} k^{-5/3}; H(k) \sim C_H \delta \varepsilon^{-1/3} k^{-5/3}, \quad (3)$$

where  $C_E$  and  $C_H$  are the two Kolmogorov constants. The spectra of energy and helicity are shown in Fig. 2, and the wide ranges of energy and helicity spectra consistent with scaling exponent  $-5/3$  ensure the fine resolution of the fully developed helical turbulence.

In order to separate the velocity field within a specific length scale  $L$  in physical space, the following bandpass filtering was used, which is written as

$$\hat{\mathbf{u}}_b^\perp = \frac{\sqrt{2}}{\sqrt{L}} 2\kappa^2 \exp(-\kappa^2) \hat{\mathbf{u}}(\mathbf{k}), \quad (4)$$

where  $\kappa = kL/2$ ,  $k = |\mathbf{k}|$ , and  $\mathbf{k}$  is the wave number vector.<sup>35,40</sup> The physical velocity field can be obtained through the inverse Fourier

**TABLE I.** Some flow field parameters of HIT.  $Re_\lambda$  is the Taylor microscale Reynolds number,  $\Delta$  is the grid spacing,  $\eta$  is the Kolmogorov length scale,  $\lambda$  is the transverse Taylor microscale,  $L_I$  is the longitudinal integral length scale,  $\varepsilon$  is the mean kinetic energy dissipation rate, and  $\delta$  is the mean helicity dissipation rate.

Case	Grid	$Re_\lambda$	$\Delta/\eta$	$\lambda/\eta$	$L_I/\eta$	$\varepsilon$	$\delta$
HIT	$1024^3$	341	1.52	21	102	0.10	0.30

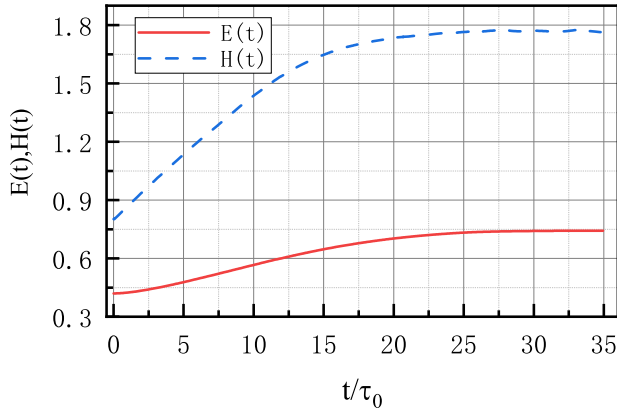


FIG. 1. The time evolution of the mean energy  $E(t)$  and the mean helicity  $H(t)$  in numerical simulations.  $\tau_0$  is the initial large-eddy turnover time.

transform on the above velocity field. The vorticity field at scale  $L$  can be computed through

$$\omega^L = \nabla \times \mathbf{u}^L. \quad (5)$$

The above filtering method separates the turbulence structures of different scales successfully, and it is sharper for  $l < L$  and less so for  $l > L$ . For scale  $l < L$ , there exists a significant dilatation of eddies, which is damped by the filter.<sup>40</sup> The bandpass filtering method has been employed to analyze the geometry and interaction of turbulence structures,<sup>40</sup> the energy cascade in real space,<sup>35</sup> and the generation and flux of enstrophy in HIT.<sup>41</sup> In addition, the bandpass filtering method with other expressions was also used to study the scale locality of the energy cascade in physical and spectral space. Verma *et al.*<sup>12</sup> investigated the shell-to-shell energy transfer rate in spectral space by expanding it to first order in perturbation. Sharp spectral filters were generalized to smooth filters and verified that a minor discrepancy exists for different definitions of scales of motions.<sup>7,8</sup> Sharp spectral filters were also employed to define a specific scale of

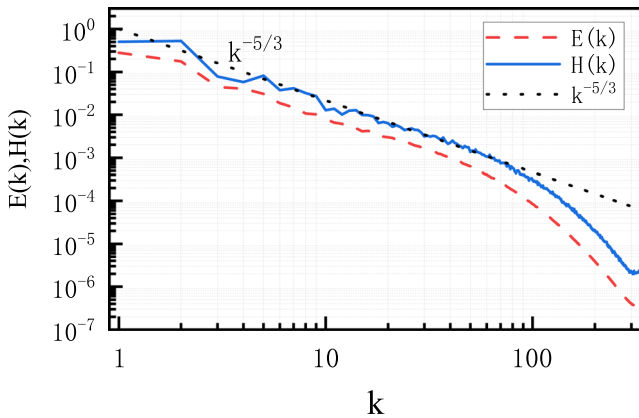


FIG. 2. Spectra of energy and helicity.

motions to estimate the effect of Reynolds number on the scale locality properties of the energy cascade.<sup>28</sup> Eyink and Aluie<sup>23</sup> and Aluie and Eyink<sup>24</sup> defined a band-passed kinetic energy density between two length scales, based on the low-pass filter method, and derived the rigorous upper bounds on the contributions of nonlocal triads.

The velocity and vorticity fields extracted to different length scales are prerequisites for further scale-to-scale energy and helicity transfer in physical space. The velocity and vorticity fields can be decomposed into large and small length scales as

$$\mathbf{u} = \mathbf{u}^L + \mathbf{u}^S, \omega = \omega^L + \omega^S, \quad (6)$$

where the superscripts  $L$  and  $S$  denote the large and small length scales, respectively. Hence, we can deduce the governing equations of the ensemble averaged large-scale and small-scale energy as<sup>35,41</sup>

$$\frac{\partial}{\partial t} \left\langle \frac{1}{2} (\mathbf{u}^L)^2 \right\rangle = -\Pi_{\Delta}^{E,L \rightarrow S} - \nu \langle (\omega^L)^2 \rangle, \quad (7)$$

$$\frac{\partial}{\partial t} \left\langle \frac{1}{2} (\mathbf{u}^S)^2 \right\rangle = \Pi_{\Delta}^{E,L \rightarrow S} - \nu \langle (\omega^S)^2 \rangle. \quad (8)$$

Here, the energy transfer function from large to small scales is

$$\Pi_{\Delta}^{E,L \rightarrow S} = \left\langle -u_i^S u_j^S \frac{\partial u_i^L}{\partial x_j} + u_i^L u_j^L \frac{\partial u_i^S}{\partial x_j} \right\rangle. \quad (9)$$

The governing equations of the ensemble averaged enstrophy at large and small scales in three-dimensional flows are

$$\frac{\partial}{\partial t} \left\langle \frac{1}{2} (\omega^L)^2 \right\rangle = -\Pi_{\Delta}^{W,L \rightarrow S} + G^L - \nu \langle (\nabla \times \omega^L)^2 \rangle, \quad (10)$$

$$\frac{\partial}{\partial t} \left\langle \frac{1}{2} (\omega^S)^2 \right\rangle = \Pi_{\Delta}^{W,L \rightarrow S} + G^S - \nu \langle (\nabla \times \omega^S)^2 \rangle, \quad (11)$$

where the cross-scale transfer term

$$\Pi_{\Delta}^{W,L \rightarrow S} = \langle \omega^L \cdot (\mathbf{u} \cdot \nabla \omega^S) \rangle = -\langle \omega^S \cdot (\mathbf{u} \cdot \nabla \omega^L) \rangle \quad (12)$$

and the source term

$$G^L = \langle \omega^L \cdot (\omega \cdot \nabla \mathbf{u}) \rangle, \quad (13)$$

$$G^S = \langle \omega^S \cdot (\omega \cdot \nabla \mathbf{u}) \rangle. \quad (14)$$

$G^L$  and  $G^S$  in the above equations represent the generations of enstrophy by vortex stretching at large and small scales.

Similarly, the governing equations of the ensemble averaged large-scale and small-scale helicity read as

$$\frac{\partial}{\partial t} \langle \mathbf{u}^L \cdot \omega^L \rangle = -\Pi_{\Delta}^{H,L \rightarrow S} - \left\langle 2\nu \frac{\partial u_i^L}{\partial x_j} \frac{\partial \omega_i^L}{\partial x_j} \right\rangle, \quad (15)$$

$$\frac{\partial}{\partial t} \langle \mathbf{u}^S \cdot \omega^S \rangle = \Pi_{\Delta}^{H,L \rightarrow S} - \left\langle 2\nu \frac{\partial u_i^S}{\partial x_j} \frac{\partial \omega_i^S}{\partial x_j} \right\rangle, \quad (16)$$

and the helicity transfer function from large to small scales defines

$$\Pi_{\Delta}^{H,L \rightarrow S} = \Pi_{\Delta}^{AD,L \rightarrow S} + \Pi_{\Delta}^{VS,L \rightarrow S}, \quad (17)$$

where

$$\Pi_{\Delta}^{AD,L \rightarrow S} = \left\langle \omega_i^L (u_j^L + u_j^S) \frac{\partial u_i^S}{\partial x_j} + u_i^L (u_j^L + u_j^S) \frac{\partial \omega_i^S}{\partial x_j} \right\rangle, \quad (18a)$$

$$\Pi_{\Delta}^{VS,L \rightarrow S} = \left\langle -u_i^L (\omega_j^L + \omega_j^S) \frac{\partial u_i^S}{\partial x_j} \right\rangle. \quad (18b)$$

The methodology of the above derivation process is similar to our previous dual-channel helicity cascade theory.<sup>42</sup>

The conservative feature of the cross-scale helicity transfer on the right-hand side of Eqs. (15) and (16) confirms that helicity is an inviscid invariant in three-dimensional turbulence. However, the governing equations of the ensemble averaged large-scale and small-scale enstrophy do not possess the cross-scale conservative feature, which indicates that the enstrophy is not an inviscid invariant in three-dimensional turbulence. The conservative helicity cascade can be decomposed into an advection term by velocity and vorticity ( $\Pi_{\Delta}^{AD,L \rightarrow S}$ ) and a vortex stretching term ( $\Pi_{\Delta}^{VS,L \rightarrow S}$ ). Note that the advection by vorticity leads to a conservative cross-scale enstrophy transfer, but the vortex stretching serves as a source in three-dimensional turbulent flows.

From the perspective of physical space, vortex stretching is the main mechanism of the energy cascade, but there is a lack of rigorous evidence to support this phenomenological picture.<sup>30</sup> It is the vortex stretching that destroys the conservative characteristics of the enstrophy cascade in three-dimensional flows.<sup>41</sup> Previous interpretations of the helicity cascade based on the filtering approach state that the skew-strain plays an important role.<sup>11</sup> Recently, the dual-channel helicity cascade theory we proposed illustrated that the vortex stretching is also involved in the helicity cascade process, which is reflected in the definition of the second channel of the helicity cascade.<sup>42</sup> Benefiting from the bandpass filtering method, we can also prove that the vortex stretching is involved in the definition of cross-scale helicity transfer Eq. (17) in physical space. Therefore, we summarize that (i) vortex stretching has been proven as a direct evidence to play an essential role in the helicity cascade process in physical space and (ii) vortex stretching, together with velocity and vorticity advections, constitutes the dynamical helicity cascade.

Next, we provide some numerical results of the cross-scale transfer functions of energy and helicity in HIT. In classical turbulent cascade theory, the forward cascade denotes the energy transfers from large scales to small scales and the backscatter cascade denotes the energy transfers from small scales to large scales. The notation also applies to the helicity cascade. In Fig. 3, we supply the numerical results of cross-scale transfer functions of energy and helicity on different ratios of the analyzed two scales, for both forward cascade and backscatter cascade. The peak and valley locations, which reflect the characteristics of the scale locality, are summarized in Table II. For the forward energy cascade, the numerical results in Fig. 3(a) confirm the conclusion that the structures of a specific length scale  $L$  mostly transfer their energy to the structures of length scale  $0.3L$ .<sup>35</sup> The peak locations in helical turbulence are somewhat lower than the results at adjacent scales reported in the literature,<sup>35</sup>

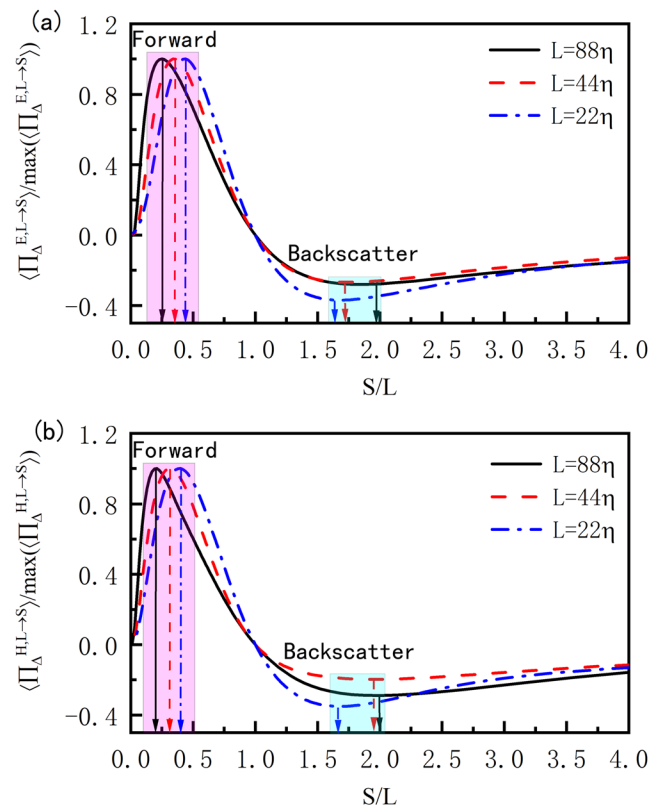


**FIG. 3.** Ensemble averages of the normalized energy transfer function (a) and the helicity transfer function (b) at different length scales. The peak values of the ensemble averages of the cross-scale transfer functions of energy and helicity are selected as the  $\max(\langle \Pi_{\Delta}^{E,L \rightarrow S} \rangle)$  and  $\max(\langle \Pi_{\Delta}^{H,L \rightarrow S} \rangle)$ , respectively.

which reflects a lower locality of the energy cascade under the broken mirror symmetry. Besides, scale locality exists in the backscatter energy cascade procedure, and the structures of a specific length scale  $L$  mostly transfer their energy in reverse to the structures of length scale  $1.5L-2L$ .

We previously assumed that the helicity cascade is less local because the locality condition of the vorticity gradient is more stringent than that of the velocity gradient in the energy cascade process,<sup>10</sup> and the direct numerical evidence shown in Fig. 3(b) confirms this assumption. In contrast with energy cascades at the same scales in Table II, the peak locations of the forward helicity cascade are

**TABLE II.** The peak locations of forward and backscatter energy and helicity cascades.

	Forward			Backscatter		
	$L = 88\eta$	$L = 44\eta$	$L = 22\eta$	$L = 88\eta$	$L = 44\eta$	$L = 22\eta$
Energy	0.25	0.34	0.44	1.88	1.73	1.67
Helicity	0.21	0.32	0.40	2.00	1.94	1.68



lower than those of the forward energy cascade, and the valley locations of the backscatter helicity cascade are deeper than those of the backward energy cascade, which reflects the weaker scale locality of the helicity cascade. In addition, the structures of a specific length scale  $L$  mostly transfer their helicity in reverse to structures of length scale  $1.5L$ – $2L$  in the inertial subrange. Therefore, we conclude that the scale locality ranges of forward and backscatter helicity cascades are broader than those of energy cascades. When adopting the multi-scale gradient expansion method for the helicity cascade,<sup>11</sup> more scales should be involved in the truncation of the helicity flux.

The adopted bandpass filtering method was used to provide local spatial geometry and morphology of turbulent structures and verified that the small-scale structures tend to cluster around a 3–5 times larger scale.<sup>35,40</sup> Leung, Swaminathan, and Davidson<sup>40</sup> proposed that the general shape and spatial distribution are not drastically altered by adopting a different threshold and suggested that a value of  $m + 1.5\sigma$  ( $m$  denotes the mean and  $\sigma$  denotes variation) can be selected as the threshold. Here, we also select the value  $m + 1.5\sigma$  as the threshold to investigate the local spatial distribution of the helicity cascade. The traditional helicity flux defined by a low-pass filter describes the helicity transfer across a specific scale  $L$ ,<sup>42</sup> and only a portion can transfer to a specific scale  $S$ . We denote the overlap regions where both the traditional helicity flux and present bandpass filtered helicity flux are larger than a threshold  $m + 1.5\sigma$  as the helicity flux from scale  $L = 44\eta$  to  $S = 14\eta$ . We show the iso-surface of the traditional helicity flux with filter width  $L = 44\eta$  in Fig. 4(a) and the iso-surface of the helicity flux from scale  $L = 44\eta$  to  $S = 14\eta$  in Fig. 4(b). The analyzed two scales correspond to the peak location of the red dashed line in Fig. 3(b). The overlap regions in Fig. 4(b) correspond to the spatial information with helicity transfer between two specific scales extracted from the traditional helicity flux. It reflects the main spatial-distribution characteristic and the scale information of the traditional helicity flux. The overlap regions tend to form clusters, and they are closely associated with the spatial distributions of large-scale and small helicity structures.

The two contributions to the conservative helicity cascade [Eqs. (18a) and (18b)] at three typical scales are numerically investigated in Fig. 5. Although the numerical results in Fig. 5 are similar to those in Fig. 3, their definitions imply that both of them could

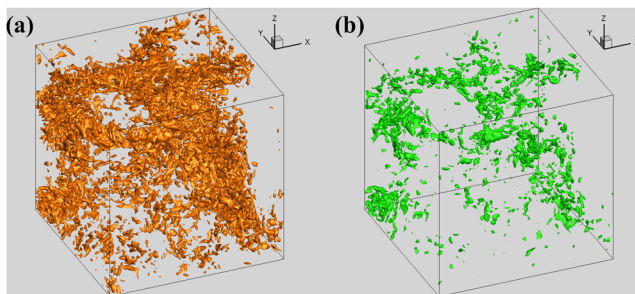


**FIG. 4.** (a) Iso-surface of traditional helicity flux  $\Pi_{\Delta}^H$  defined by a low-pass filter with filter width  $L = 44\eta$ . (b) Iso-surface of overlap regions of traditional helicity flux  $\Pi_{\Delta}^H$  defined by a low-pass filter with filter width  $L = 44\eta$  and the present helicity flux  $\Pi_{\Delta}^{H,L \rightarrow S}$  defined by a bandpass filter with scale  $L = 44\eta$  and  $S = 14\eta$ .

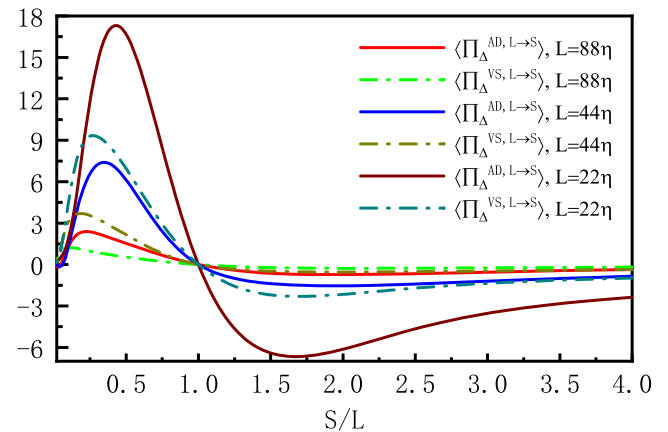


**FIG. 5.** Ensemble averages of two helicity transfer functions at different length scales.

lead to a conservative helicity cascade. The amplitudes of the ensemble averages of the advection term Eq. (18a) are always larger than those of the vortex stretching term [Eq. (18b)] for both forward and backscatter helicity cascades, which means that the vortex stretching term plays a secondary role in the helicity cascade process in physical space. In addition, the local helicity transfer at relatively small scales is still strong, which is reflected in the larger amplitudes at small scales in Fig. 3. The regulation of a local stronger helicity cascade at small scales is consistent with the previous conclusions that the local energy cascade at small scales is very strong.<sup>43</sup> In contrast to the statistical analysis based on filtering methods, this scale decomposition method provides more statistical evidence of the specific underlying physical mechanism.

The scale locality of energy and helicity cascades in physical space was theoretically and numerically investigated. We employed the scale decomposition method to derive an exact expression for the conservative helicity transfer in physical space. It has been rigorously proven that vortex stretching plays an essential role in the helicity cascade process, although it is secondary to the advection term by velocity and vorticity. However, vortex stretching is associated with the energy cascade and breaks the conservative characteristic of enstrophy transfer in three-dimensional flows. Although a turbulent structure of scale  $L$  will also transfer most of its helicity to smaller scales of around  $0.3L$ , the scale locality of the helicity cascade is slightly weaker than that of the energy cascade. Hence, in broken reflection-symmetric flows, the scale locality of the energy and helicity cascades will be weaker, and more scales should be involved in modeling the turbulent cascade of helical turbulence.

This work was supported by the National Key Research and Development Program of China (Grant Nos. 2019YFA0405300 and 2016YFA0401200), the National Natural Science Foundation of China (NSFC Grant No. 91852203), the Science Challenge Project (Grant No. TZ2016001), and the Strategic Priority Research Program of Chinese Academy of Sciences (Grant No. XDC01000000). The authors thank the National Supercomputer Center in Tianjin (NSCC-TJ) and the National Supercomputer Center in Guangzhou (NSCC-GZ) for providing computer time.

## DATA AVAILABILITY

The data that support the findings of this study are available from the corresponding author upon reasonable request.

## REFERENCES

- <sup>1</sup>U. Frisch, *Turbulence: The Legacy of A. N. Kolmogorov* (Cambridge University Press, Cambridge, England, 1995).
- <sup>2</sup>A. N. Kolmogorov, "The local structure of turbulence in incompressible viscous fluid for very large Reynolds number," *Dokl. Akad. Nauk SSSR* **30**, 299–303 (1941).
- <sup>3</sup>R. H. Kraichnan, "The structure of isotropic turbulence at very high Reynolds numbers," *J. Fluid Mech.* **5**, 497–543 (1959).
- <sup>4</sup>A. Alexakis and L. Biferale, "Cascades and transitions in turbulent flows," *Phys. Rep.* **767–769**, 1–101 (2018).
- <sup>5</sup>P. K. Yeung and J. G. Brasseur, "The response of isotropic turbulence to isotropic and anisotropic forcing at the large scales," *Phys. Fluids A* **3**, 884–897 (1991).
- <sup>6</sup>J. A. Domaradzki, W. Liu, and M. E. Brachet, "An analysis of subgrid-scale interactions in numerically simulated isotropic turbulence," *Phys. Fluids A* **5**, 1747 (1993).
- <sup>7</sup>J. A. Domaradzki and D. Carati, "An analysis of the energy transfer and the locality of nonlinear interactions in turbulence," *Phys. Fluids* **19**, 085112 (2007).
- <sup>8</sup>J. A. Domaradzki and D. Carati, "A comparison of spectral sharp and smooth filters in the analysis of nonlinear interactions and energy transfer in turbulence," *Phys. Fluids* **19**, 085111 (2007).
- <sup>9</sup>G. L. Eyink, "Energy dissipation without viscosity in ideal hydrodynamics. I. Fourier analysis and local energy transfer," *Physica D* **78**, 222–240 (1994).
- <sup>10</sup>G. L. Eyink, "Locality of turbulent cascades," *Physica D* **207**, 91–116 (2005).
- <sup>11</sup>G. L. Eyink, "Multi-scale gradient expansion of the turbulent stress tensor," *J. Fluid Mech.* **549**, 159–190 (2006).
- <sup>12</sup>M. K. Verma, A. Ayyer, O. Deblieux, S. Kumar, and A. V. Chandra, "Local shell-to-shell energy transfer via nonlocal interactions in fluid turbulence," *Pramana* **65**, 297–310 (2005).
- <sup>13</sup>A. Alexakis, P. D. Mininni, and A. Pouquet, "Imprint of large-scale flows on turbulence," *Phys. Rev. Lett.* **95**, 264503 (2005).
- <sup>14</sup>P. D. Mininni, A. Alexakis, and A. Pouquet, "Nonlocal interactions in hydrodynamic turbulence at high Reynolds numbers: The slow emergence of scaling laws," *Phys. Rev. E* **77**, 036306 (2008).
- <sup>15</sup>J. I. Cardesa, A. Vela-Martín, S. Dong, and J. Jiménez, "The temporal evolution of the energy flux across scales in homogeneous turbulence," *Phys. Fluids* **27**, 111702 (2015).
- <sup>16</sup>J. I. Cardesa, A. Vela-Martín, and J. Jiménez, "The turbulent cascade in five dimensions," *Science* **357**, 782–784 (2017).
- <sup>17</sup>M. Buzzicotti, M. Linkmann, H. Aluie, L. Biferale, J. Brasseur, and C. Meneveau, "Effect of filter type on the statistics of energy transfer between resolved and subfilter scales from *a-priori* analysis of direct numerical simulations of isotropic turbulence," *J. Turbul.* **19**, 167–197 (2018).
- <sup>18</sup>D. Zhao and H. Aluie, "Inviscid criterion for decomposing scales," *Phys. Rev. Fluids* **3**, 054603 (2018).
- <sup>19</sup>F. Cadieux and J. A. Domaradzki, "Periodic filtering as a subgrid-scale model for LES of laminar separation bubble flows," *J. Turbul.* **17**, 954–965 (2016).
- <sup>20</sup>H. Aluie and G. L. Eyink, "Scale locality of magnetohydrodynamic turbulence," *Phys. Rev. Lett.* **104**, 081101 (2010).
- <sup>21</sup>Y. Yang, Y. Shi, M. Wan, W. H. Matthaeus, and S. Chen, "Energy cascade and its locality in compressible magnetohydrodynamic turbulence," *Phys. Rev. E* **93**, 061102 (2016).
- <sup>22</sup>H. Aluie, "Compressible turbulence: The cascade and its locality," *Phys. Rev. Lett.* **106**, 174502 (2011).
- <sup>23</sup>G. L. Eyink and H. Aluie, "Localness of energy cascade in hydrodynamic turbulence. I. Smooth coarse graining," *Phys. Fluids* **21**, 115107 (2009).
- <sup>24</sup>H. Aluie and G. L. Eyink, "Localness of energy cascade in hydrodynamic turbulence. II. Sharp spectral filter," *Phys. Fluids* **21**, 115108 (2009).
- <sup>25</sup>V. L'vov and G. Falkovich, "Counterbalanced interaction locality of developed hydrodynamic turbulence," *Phys. Rev. A* **46**, 4762–4772 (1992).
- <sup>26</sup>Y. Zhou, "Degrees of locality of energy transfer in the inertial range," *Phys. Fluids A* **5**, 1092–1094 (1993).
- <sup>27</sup>Y. Zhou, "Interacting scales and energy transfer in isotropic turbulence," *Phys. Fluids A* **5**, 2511–2524 (1993).
- <sup>28</sup>J. A. Domaradzki, B. Teaca, and D. Carati, "Locality properties of the energy flux in turbulence," *Phys. Fluids* **21**, 025106 (2009).
- <sup>29</sup>P. A. Davidson, *Turbulence: An Introduction for Scientists and Engineers* (Oxford University Press, Oxford, 2015).
- <sup>30</sup>G. Sahoo, M. De Pietro, and L. Biferale, "Helicity statistics in homogeneous and isotropic turbulence and turbulence models," *Phys. Rev. Fluids* **2**, 024601 (2017).
- <sup>31</sup>R. Betchov, "An inequality concerning the production of vorticity in isotropic turbulence," *J. Fluid Mech.* **1**, 497–504 (1956).
- <sup>32</sup>W. T. Ashurst, A. R. Kerstein, R. M. Kerr, and C. H. Gibson, "Alignment of vorticity and scalar gradient with strain rate in simulated Navier–Stokes turbulence," *Phys. Fluids* **30**, 2343–2353 (1987).
- <sup>33</sup>K. Yoshimatsu, K. Anayama, and Y. Kaneda, "Influence of vortex dynamics and structure on turbulence statistics at large scales," *Phys. Fluids* **27**, 055106 (2015).
- <sup>34</sup>L. K. Su and W. J. A. Dahm, "Scalar imaging velocimetry measurements of the velocity gradient tensor field in turbulent flows. I. Assessment of errors," *Phys. Fluids* **8**, 1869–1882 (1996).
- <sup>35</sup>N. A. K. Doan, N. Swaminathan, and P. A. Davidson, "Scale locality of the energy cascade using real space quantities," *Phys. Rev. Fluids* **3**, 084601 (2018).
- <sup>36</sup>B. Galanti and A. Tsinober, "Physical space properties of helicity in quasi-homogeneous forced turbulence," *Phys. Lett. A* **352**, 141–149 (2006).
- <sup>37</sup>A. S. Teimurazov, R. A. Stepanov, M. K. Verma, S. Barman, A. Kumar, and S. Sadhukhan, "Direct numerical simulation of homogeneous isotropic helical turbulence with the TARANG code," *J. Appl. Mech. Tech. Phys.* **59**, 1279–1287 (2018).
- <sup>38</sup>Z. Yan, X. Li, J. Wang, and C. Yu, "Effect of pressure on joint cascade of kinetic energy and helicity in compressible helical turbulence," *Phys. Rev. E* **99**, 033114 (2019).
- <sup>39</sup>Q. Chen, S. Chen, and G. L. Eyink, "The joint cascade of energy and helicity in three-dimensional turbulence," *Phys. Fluids* **15**, 361–374 (2003).
- <sup>40</sup>T. Leung, N. Swaminathan, and P. A. Davidson, "Geometry and interaction of structures in homogeneous isotropic turbulence," *J. Fluid Mech.* **710**, 453 (2012).
- <sup>41</sup>P. A. Davidson, K. Morishita, and Y. Kaneda, "On the generation and flux of enstrophy in isotropic turbulence," *J. Turbul.* **9**, N42 (2008).
- <sup>42</sup>Z. Yan, X. Li, C. Yu, J. Wang, and S. Chen, "Dual channels of helicity cascade in turbulent flows," *J. Fluid Mech.* **894**, R2 (2020).
- <sup>43</sup>D. Kuzzay, A. Alexandrova, and L. Matteini, "Local approach to the study of energy transfers in incompressible magnetohydrodynamic turbulence," *Phys. Rev. E* **99**, 053202 (2019).